

Groundwater processes in Hebes Chasma, Mars

Peter M. Grindrod^{1,2} and Matthew R. Balme^{3,4}

Received 27 May 2010; accepted 14 June 2010; published 15 July 2010.

[1] We describe a conceptual model of groundwater processes at Hebes Chasma, Mars, which can account for the distribution of hydrated minerals and their subsequent evolution. At Hebes Chasma, pressure gradients set up by the large central mound, Hebes Mensa, could cause groundwater to be sourced predominantly from beneath the central region, if such water were present. Evaporation of upwelling groundwater would cause monohydrates to form at or near the surface through efflorescence, and polyhydrates to form inside the central mound through subflorescence. This crystallization could lead to an excess pore pressure, causing large-scale weakening and subsequent collapse that can reveal the interior polyhydrated deposits. If evaporation is high compared to groundwater inflow, then increased crystallization would promote the formation of collapse zones. If evaporation is low compared to groundwater inflow then there would be a greater chance for water reaching the surface and the possible formation of karst landforms. **Citation:** Grindrod, P. M., and M. R. Balme (2010), Groundwater processes in Hebes Chasma, Mars, *Geophys. Res. Lett.*, 37, L13202, doi:10.1029/2010GL044122.

1. Introduction

[2] Hebes Chasma is an approximately elliptical closed depression measuring 315 by 125 km, located about 300 km to the north of the main Valles Marineris chasmata system. Hebes Chasma is one of the deepest canyon systems on Mars, with a maximum depth of about 9 km. Inside Hebes Chasma is a distinctive layered central mound, Hebes Mensa, that mimics the elongation of the Chasma. The mensa is one of about ten large-scale interior layered deposits (ILDs) that occur in the Valles Marineris chasmata system [e.g., *Lucchitta et al.*, 1992], whose formation mechanism remain a matter of ongoing debate [e.g., *Adams et al.*, 2009; *Montgomery et al.*, 2009; *Fueten et al.*, 2006; *Okubo et al.*, 2008]. Here we do not address how Hebes Chasma or Hebes Mensa formed, as to a large extent the processes we discuss are unaffected by the original formation mechanism. Instead, we investigate the implications of recent studies highlighting the possible importance of groundwater on Mars, from in situ [e.g., *Squyres et al.*, 2006] and orbital [e.g., *Murchie et al.*, 2009] observations and hydrological models [e.g., *Andrews-Hanna et al.*, 2007]. We describe a conceptual

model of groundwater processes in Hebes Chasma, which is split into two parts: (1) modeling the pressure gradients caused by the topography in order to predict possible upwelling locations, and (2) applying the results of previous crystallization experiments to Martian conditions in order to predict crystallization processes. We present evidence to support this combined model of groundwater upwelling and evaporation, and discuss the implications for other ILDs on Mars.

2. Groundwater Processes in Hebes Chasma

2.1. Topographic Pumping

[3] Any groundwater present beneath the wider region around Hebes Chasma will naturally be driven by the surrounding topography towards the lowest point at the surface, in a process analogous to basin recharge on Earth. However, to investigate the pattern of any possible groundwater upwelling near Hebes Mensa, we model the pressure-gradients created by the topography of Hebes Chasma both with and without Hebes Mensa. We apply to Hebes Chasma the topographic pumping model of *Showman et al.* [2004], which is based on the topographic relaxation model of *Turcotte and Schubert* [2002], to predict the subsurface stress field available to drive a fluid through a porous matrix. We assume throughout that the rock density is 3000 kg m^{-3} and acceleration due to gravity is 3.7 ms^{-2} , and consider two specific topographic cases. We first approximate the minor axis topography of Hebes Chasma in the absence of Hebes Mensa by assuming a sinusoidal surface topography of wavelength 140 km and amplitude 4 km. This topographic profile creates pressure gradients that lead to a zone of upwelling $\sim 75 \text{ km}$ wide in the center of Hebes Chasma, as material flows down pressure gradients away from the walls and towards the central low region (Figure 1a). By superposing four Fourier modes, we also approximate the combined present-day topography of Hebes Chasma and Hebes Mensa. Again, the long wavelength of Hebes Chasma dominates the subsurface pressure-gradients, but the addition of Hebes Mensa reduces the zone of upwelling to a central region $\sim 40 \text{ km}$ wide, and suggests that the majority of water would be sourced from below Hebes Mensa, rather than from the canyon walls (Figure 1b). Although it is likely that topographic pumping is not the only groundwater driving force, other processes such as capillary action or brine reflux will probably be secondary in magnitude and operate only in the upper tens of meters of the subsurface [e.g., *Warren*, 2006; *Scherer*, 2004].

2.2. Crystallization Effects

[4] Any groundwater rising towards the surface would begin to evaporate as it encountered the low-pressure Martian atmosphere, leading to the crystallization of any dissolved species. The process of groundwater upwelling and evaporation

¹Department of Earth Sciences, University College London, London, UK.

²Centre for Planetary Sciences, University College London, London, UK.

³Department of Earth and Environmental Sciences, Open University, Milton Keynes, UK.

⁴Planetary Science Institute Tucson, Tucson, Arizona, USA.

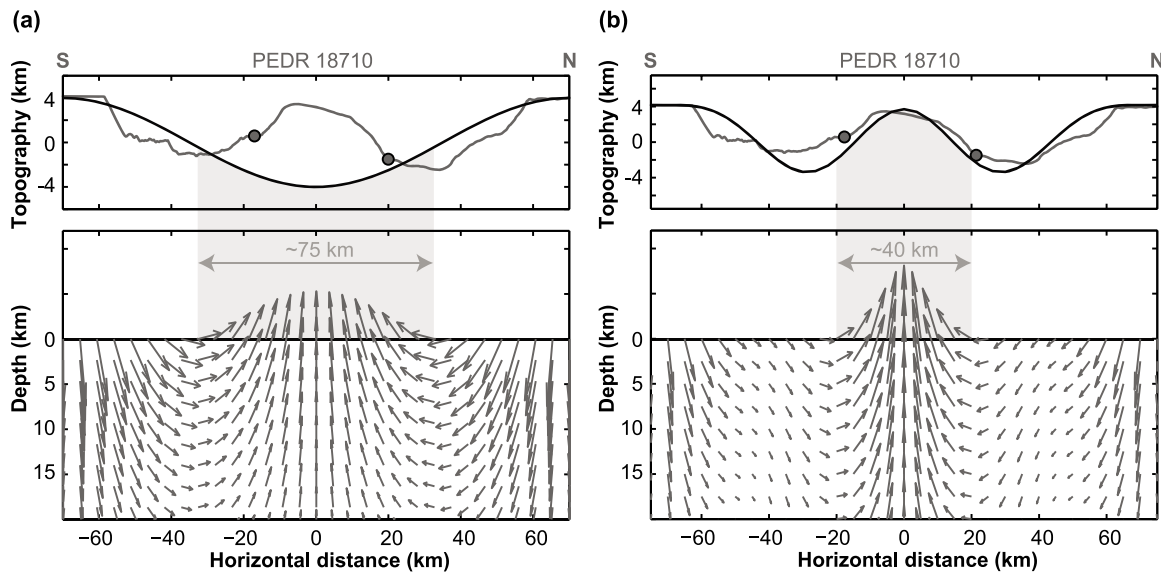


Figure 1. Results of the topographic pumping model. (a) Model topography made with a single sinusoid to represent Hebes Chasma without a central mound. (b) Model topography made with several superposed Fourier modes to represent Hebes Chasma with a central mound. In both cases the top plot shows the input topography (black line), an example of the real topography (gray line) taken from MOLA profile 18710, and the location of the base of the ILDs in Hebes Mensa (solid circles). In each case the bottom plot shows the pressure gradients (arrows) caused by the modeled topography and the zone of upwelling at the surface (gray arrow and block).

would leave a distinctive pattern of crystallization that varies with depth and location in the central Hebes mound. At the low-pressure surface, evaporation will cause the groundwater to become supersaturated, and thus precipitation of primary salts occurs through efflorescence, a process common in building stones on Earth [e.g., Scherer, 2004]. The first salts to crystallize through efflorescence at the low relative humidity surface will be anhydrous, such as anhydrite (CaSO_4), or low hydrates, such as monohydrates like kieserite ($\text{MgSO}_4 \cdot \text{H}_2\text{O}$) [e.g., Chou and Seal, 2007]. The higher relative humidity inside the central mound will result in the crystallization of polyhydrated minerals, such as epsomite ($\text{MgSO}_4 \cdot 7\text{H}_2\text{O}$) and mirabilite ($\text{Na}_2\text{SO}_4 \cdot 10\text{H}_2\text{O}$), through subflorescence, or crystallization below the surface [e.g., Rodriguez-Navarro and Doehne, 1999]. However, this zoning might be offset to a certain extent by any temperature gradient between the surface and interior of the mound, as polyhydrates tend to form at lower temperatures [e.g., Peterson and Wang, 2006]. But as long as evaporation dominates over any temperature effect, as would likely be the case in an atmosphere similar to that of present-day Mars, then groundwater-driven crystallization would result in distinct zones of hydration: anhydrites and monohydrates at the surface through efflorescence, and polyhydrates in the interior through subflorescence.

[5] The crystallization of salt can lead to significant stress damage in porous rocks [e.g., Scherer, 2004; Steiger et al., 2008]. A crystal growing in a supersaturated solution within a confined pore space will exert a pressure on the surrounding matrix. These stresses are often sufficient to cause failure in tension of the host rock, especially if there are repeated cycles of evaporation [e.g., Steiger and Asmussen, 2008]. For example, in the sodium sulfate-water system, crystallization pressures are higher at lower temperatures, and at 0°C can be as high as 37 or 27 MPa in mirabilite or the metastable

heptahydrate ($\text{Na}_2\text{SO}_4 \cdot 7\text{H}_2\text{O}$) respectively [Steiger and Asmussen, 2008]. Although this pressure is exerted at the scale of the pores, if a large fraction of the crystals are in contact with their pore walls, and if the matrix is saturated with groundwater, then the crystallization pressures can be directly compared with the tensile strength of the rock matrix [Steiger and Asmussen, 2008]. The tensile strength of rocks is of the order of one-tenth of the uniaxial compressive strength (UCS), and so has an upper limit of about 30 MPa, but can vary due to a number of factors, including composition, porosity, alteration, and stress history [Paterson and Wong, 2005]. For example, the tensile strength of sandstone can vary from less than 1 MPa up to 20 MPa [e.g., Bell, 1999]. The tensile strength of Martian sulfate hydrates is unknown, but analog materials have UCS values of up to about 70 MPa, depending on porosity [Grindrod et al., 2010]. Regardless of the exact tensile strength of any particular rock mass that makes up Hebes Montes, it is clear that under the right conditions, the stress generated through the crystallization of salts is capable of causing rock damage, and subsequent fracture and collapse. In fact, as higher crystallization pressures are generally the result of precipitation of the highest hydrates, then it is possible that failure in coherent planes of polyhydrated subflorescence layers in the interior of Hebes Montes could be more important than at the surface, causing large-scale collapse.

3. Observational Evidence of Groundwater Action

[6] Observational evidence of possible groundwater action is confined to Hebes Mensa and its immediate vicinity, supporting the idea of upwelling being confined to the central region of Hebes Chasma. We have found no evidence for groundwater action on the chasma walls. The N-S distance

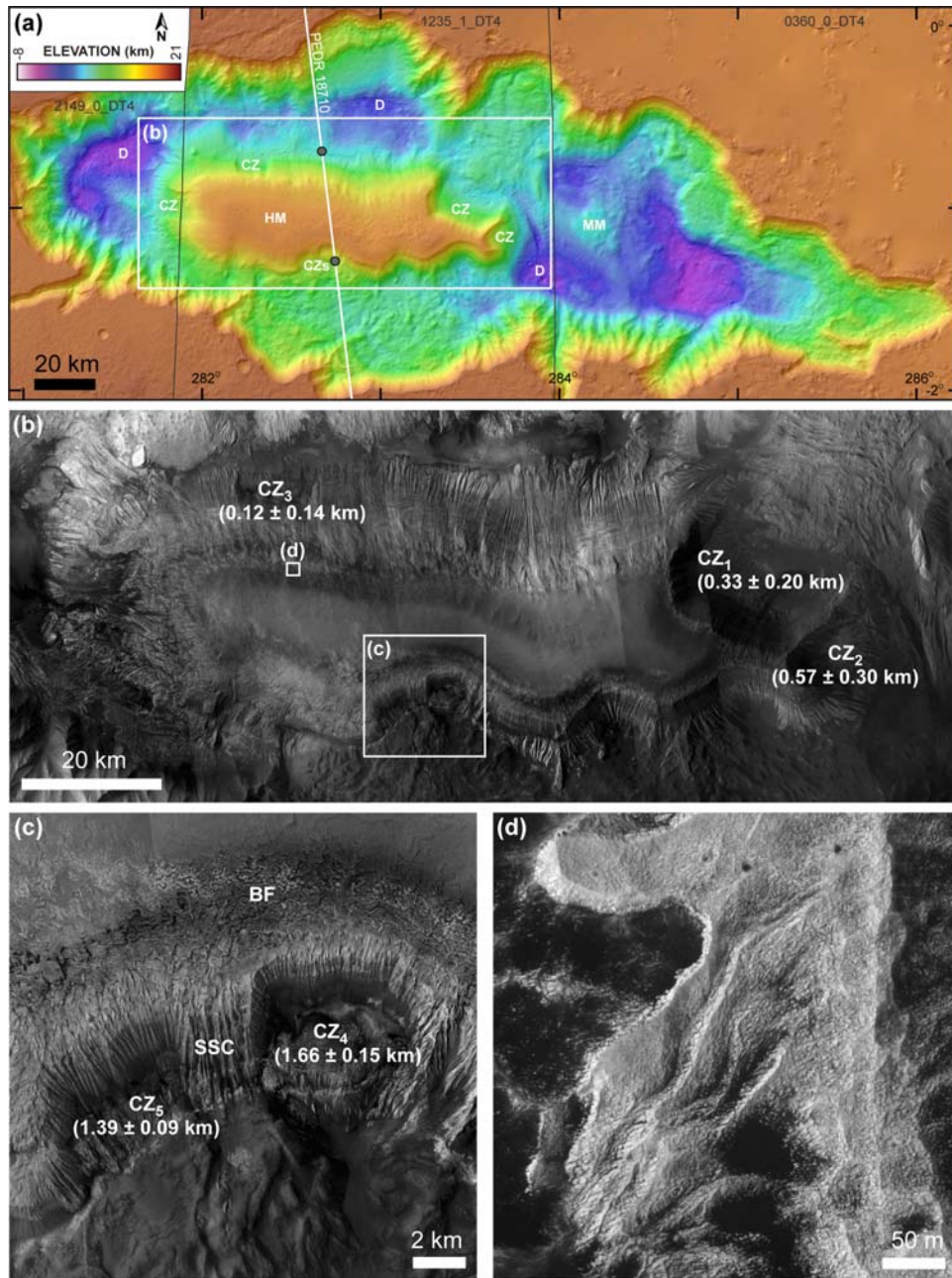


Figure 2. Evidence of groundwater processes in Hebes Mensa. (a) Topographic map of Hebes Chasma showing the location of a subsequent image and MOLA profile 18710. Solid circles show the location of the base of the ILDs shown in Figure 1. Features discussed in the text include Hebes Mensa (HM), “mini-Mensa” (MM), collapse zone (CZ) and depression (D). Made from HRSC topography, with image numbers given at the top. (b) CTX image mosaic of the general Hebes Mensa region with location of higher resolution images (white boxes). The mean height of each collapse zone plane ± 1 s.d. is given in brackets. (c) Part of south Hebes Mensa showing two large-scale collapse zones, near-summit botryoidal features (BF), and small-scale channels (SSCs). CTX images P13_006164_1791 and P_15_007021_1777. (d) Sinuous SSCs in light-toned material near the summit of Hebes Mensa. HiRISE image PSP_005808_1790.

across Hebes Mensa from the base of the ILDs is $\sim 35\text{--}45$ km, matching well with the location of upwelling predicted by the pressure gradients when a central mound is included. The exact locations of the base of the ILDs in the north and south of Hebes Mensa are obscured in most places by mantling sand dunes and sheets and some landslide deposits, but have elevations of roughly -1.5 and 0 km respectively, suggesting local variations in upwelling, possibly as a result of variations in initial topography. Hebes Mensa has at least five large

zones of collapse (Figure 2), ranging from 6 to 23 km in width, which have each removed areas of up to about 290 km^2 from the main mensa, amounting to a total of approximately 550 km^2 of removal. In many cases, extensive hummocky terrain extends from the base of the collapse zones, suggesting the possible run-out and emplacement of debris (either wet or dry [e.g., Legros, 2002; Soukhovitskaya and Manga, 2006]). The mean elevation of each collapse plane suggests two different elevations: one at $\sim 0.1\text{--}0.6$ km above Mars

datum, and another at 1.4–1.7 km (Figure 2). HiRISE images show the highest density of joints possibly related to dehydration and aqueous mineral crystal growth [e.g., *Okubo and McEwen*, 2007] directly above one large collapse zone in the north of Hebes Mensa, suggesting possible groundwater action here.

[7] We divide candidate fluvial landforms in Hebes Montes into three main categories: (1) small-scale channels, (2) inverted features, and (3) large-scale channels. Numerous small-scale channels occur only on the slopes of Hebes Montes, not the chasma walls, and range from ~100 to 1000 m in width, and from less than 1 km to over 13 km in length (Figure 2b). They generally originate near the top of Hebes Mensa, at elevations of between 3 and 3.5 km, where many small (~100–300 m) scalloped depressions join to form individual parallel channels. There are several examples of low sinuosity channels, particularly at lower elevations. We have also identified several examples of a possible subset of small-scale channels near the top of Hebes Montes in a single HiRISE image (Figure 2c). These small sinuous channels are approximately 10 m wide and 300 m long, and only occur in light-toned material.

[8] Inverted features originating from Hebes Montes have previously been interpreted as spring deposits [*Rossi et al.*, 2008]. These features have positive overlapping flow topography and, in some locations, a lobate appearance. Smaller-scale inverted structures also occur towards the top of Hebes Mensa, where many individual ridges of less than 100 m in width overlap to give a botryoidal appearance [*Adams et al.*, 2009]. These features have previously been attributed to eruptive spring deposits or nested diapirs [*Adams et al.*, 2009], with similar features attributed to fluvial action in Ius Chasma [*Weitz et al.*, 2010].

[9] The large-scale channels are the least numerous, but have the most well-defined erosional morphologies. The best example, occurring to the east of Hebes Montes, is about 3 km wide, 500 m deep, and 26 km long, and has cut through layered material in Hebes Montes to create a ‘mini-Mensa’ [*Adams et al.*, 2009]. Although there are significant amounts of dark aeolian material covering these landforms, it is evident that large-scale channels terminate in depressions (Figure 2). In at least one case, these depressions are surrounded by well-defined layered deposits.

4. Discussion

[10] It is likely that the present surface has been affected by aeolian processes during and since its formation. Most surfaces in Hebes Chasma show evidence for wind-deposition of varying degrees, and in some areas there is sufficient material to allow the formation of different types of dune. The enclosed nature of Hebes Chasma means that the removal of aeolian material from the canyon is likely to be inefficient, leading to large volumes of wind-derived material locally deposited. Wind erosion is also likely to be important in Hebes Chasma. Some of the features that we classify as small-scale channels have previously been interpreted as yardangs [*Hauber et al.*, 2008], and show similarities with aeolian erosional features in the Medusae Fossae Formation [e.g., *Ward*, 1979]. It is therefore possible that the small-scale “channels” are in fact simply examples of yardang-like features forming on steep slopes in a friable material. The observation that small-scale channels are best defined near

the base of Hebes Mensa could provide evidence that the material making up the lower portion of Hebes Montes has undergone sufficient groundwater cementation to prevent complete subsequent weathering. Increased cementation, and therefore possible precipitation of hydrated minerals, at lower elevations fits well with the observation of kieserite at several stratigraphic low locations around Hebes Mensa [*Gendrin et al.*, 2005; *Hauber et al.*, 2008; *Adams et al.*, 2009]. However, it is difficult to reconcile sinuous channels, especially those in upper Hebes Montes (Figure 2c), or large-scale channels, with a purely aeolian origin, as their morphologies are more indicative of fluid flow. Some of the small-scale channels also have similarities with features in Candor Mensa recently interpreted as fluvial in origin [*Murchie et al.*, 2009], so we suggest that not all of these features can be attributed to wind erosion.

[11] If monohydrates do not alter to polyhydrates, or vice-versa [*Roach et al.*, 2009], then sulfate deposits offer an insight into the original deposition method and environment [*Murchie et al.*, 2009]. Our model of efflorescence and subflorescence (Figure S1 of the auxiliary material) can account for general observations made with recent CRISM data.¹ Polyhydrates have generally been observed to be higher in the stratigraphic section than monohydrates [e.g., *Bishop et al.*, 2009; *Murchie et al.*, 2009]. Our model of efflorescence and subflorescence can also account for such a stratigraphy, as crystallization-driven collapse would remove the outer efflorescent monohydrates, revealing the stratigraphically-higher polyhydrated interior. Monohydrates could then also overlie the polyhydrates where collapse has not yet removed the outer efflorescent layer.

[12] Although not yet reported in the Hebes region, other ILDs show evidence of monohydrates outcropping on steep slopes and polyhydrates on shallower slopes [e.g., *Murchie et al.*, 2009]. Although this observation is likely to be partly due to the inherent strength of the different hydrates [e.g., *Grindrod et al.*, 2010], crystallization-driven collapse would cause an initially steep monohydrate slope to become shallower, whilst simultaneously revealing interior polyhydrated material. This erosional scenario is supported by observations of monohydrates as the dominant sulfate phase in erosional debris in Ceti and Candor Mensae [*Murchie et al.*, 2009].

[13] The majority of morphological observations at Hebes Mensa match well with those expected from karstic processes, and already suggested for a different ILD [*Baioni and Wezel*, 2010]. Most hydrated minerals, particularly sulfates, are highly soluble, and will have a propensity to undergo chemical, as well as physical, erosion from ground or surface water. Specific features identified in Hebes Mensa are comparable to terrestrial dissolution-formed counterparts, such as the source region scalloped depressions and initial small-scale channels (decantation flutes), planar belt of no channeling (sheet flow region), distal end of small-scale channels (solution runnels), and depressions at the end of channels (large-scale solution pits: see review by *Ford and Williams* [2007]). Any hydrates at Hebes Mensa would undergo dissolution from groundwater that was not in chemical equilibrium with the phase present, and so karstic processes could occur for a wide range of water compositions. If the groundwater was at some point acidic, similar to conditions

¹Auxiliary materials are available in the HTML. doi:10.1029/2010GL044122.

suggested at Meridiani Planum [e.g., *Squyres et al.*, 2006] or Mars in general [e.g., *Burns*, 1993; *Marion et al.*, 2003], then karstic features could occur in a wider range of rock types, rather than being confined to sulfate-rich deposits. Thus, regardless of the exact nature of formation of Hebes Chasma and Mensa, groundwater could have had an important effect on the both the distribution of hydrated minerals and their subsequent evolution.

[14] **Acknowledgments.** PMG and MRB are funded by STFC Aurora Research Fellowships (grants ST/F011830/1 and ST/F012020/1 respectively).

References

- Adams, J. B., A. R. Gillespie, M. P. A. Jackson, D. R. Montgomery, T. P. Dooley, J.-P. Combe, and B. C. Schreiber (2009), Salt tectonics and collapse of Hebes Chasma, Valles Marineris, Mars, *Geology*, *37*, 691–694, doi:10.1130/G30024A.1.
- Andrews-Hanna, J. C., R. J. Phillips, and M. T. Zuber (2007), Meridiani Planum and the global hydrology of Mars, *Nature*, *446*, 163–166, doi:10.1038/nature05594.
- Baioni, D., and F. C. Wezel (2010), Morphology and origin of an evaporitic dome in the eastern Tithonium Chasma, Mars, *Planet. Space Sci.*, *58*, 847–857, doi:10.1016/j.pss.2010.01.009.
- Bell, F. G. (1999), *The Engineering Properties of Soils and Rocks*, Blackwell, Oxford, U. K.
- Bishop, J. L., et al. (2009), Mineralogy of Juventae Chasma: Sulfates in the light-toned mounds, mafic minerals in the bedrock, and hydrated silica and hydroxylated ferric sulfate on the plateau, *J. Geophys. Res.*, *114*, E00D09, doi:10.1029/2009JE003352.
- Burns, R. G. (1993), Rates and mechanisms of chemical weathering of ferromagnesian silicate minerals on Mars, *Geochim. Cosmochim. Acta*, *57*, 4555–4574, doi:10.1016/0016-7037(93)90182-V.
- Chou, I.-M., and R. R. Seal (2007), Magnesium and calcium sulfate stabilities and the water budget of Mars, *J. Geophys. Res.*, *112*, E11004, doi:10.1029/2007JE002898.
- Ford, D. C., and P. Williams (2007), *Karst Hydrogeology and Geomorphology*, John Wiley, Chichester, U. K.
- Fuente, F., R. Stesky, P. MacKinnon, E. Hauber, K. Gwinner, F. Scholten, T. Zegers, and G. Neukum (2006), A structural study of an interior layered deposit in southwestern Candor Chasma, Valles Marineris, Mars, using high-resolution stereo camera data from Mars Express, *Geophys. Res. Lett.*, *33*, L07202, doi:10.1029/2005GL025035.
- Gendrin, A., et al. (2005), Sulfates in Martian layered terrains: The OMEGA/Mars Express view, *Science*, *307*, 1587–1591, doi:10.1126/science.1109087.
- Grindrod, P. M., M. J. Heap, A. D. Fortes, P. G. Meredith, I. G. Wood, F. Trippetta, and P. R. Sammonds (2010), Experimental investigation of the mechanical properties of synthetic magnesium sulfate hydrates: Implications for the strength of hydrated deposits on Mars, *J. Geophys. Res.*, doi:10.1029/2009JE003552, in press.
- Hauber, E., et al. (2008), Hebes Chasma, Mars: Slopes and stratigraphy of interior layered deposits [CD-ROM], *Lunar Planet. Sci.*, XXXIX, Abstract 2375.
- Legros, F. (2002), The mobility of long-runout landslides, *Eng. Geol.*, *63*, 301–331, doi:10.1016/S0013-7952(01)00090-4.
- Lucchitta, B. K., A. S. McEwen, G. D. Clow, P. E. Geissler, R. B. Singer, R. A. Schultz, and S. W. Squyres (1992), The canyon system on Mars, in *Mars*, edited by H. H. Kieffer et al., pp. 53–492, Univ. of Ariz. Press, Tucson.
- Marion, G. M., D. C. Catling, and J. S. Kargel (2003), Modeling aqueous ferrous iron chemistry at low temperatures with application to Mars, *Geochim. Cosmochim. Acta*, *67*, 4251–4266, doi:10.1016/S0016-7037(03)00372-7.
- Montgomery, D. R., S. M. Som, M. P. A. Jackson, B. C. Schreiber, A. R. Gillespie, and J. B. Adams (2009), Continental-scale salt tectonics on Mars and the origin of Valles Marineris and associated outflow channels, *Geol. Soc. Am. Bull.*, *121*, 117–133, doi:10.1130/B26307.1.
- Murchie, S., et al. (2009), Evidence for the origin of layered deposits in Candor Chasma, Mars, from mineral composition and hydrologic modeling, *J. Geophys. Res.*, *114*, E00D05, doi:10.1029/2009JE003343.
- Okubo, C. H., and A. S. McEwen (2007), Fracture-controlled paleo-fluid flow in Candor Chasma, Mars, *Science*, *315*, 983–985, doi:10.1126/science.1136855.
- Okubo, C. H., K. W. Lewis, A. S. McEwen, and R. L. Kirk (2008), Relative age of interior layered deposits in southwest Candor Chasma based on high-resolution structural mapping, *J. Geophys. Res.*, *113*, E12002, doi:10.1029/2008JE003181.
- Paterson, M. S., and T.-F. Wong (2005), *Experimental Rock Deformation: The Brittle Field*, Springer, Berlin.
- Peterson, R. C., and R. Wang (2006), Crystal molds on Mars: Melting of a possible new mineral species to create Martian chaotic terrain, *Geology*, *34*, 957–960, doi:10.1130/G22678A.1.
- Roach, L. H., J. F. Mustard, S. L. Murchie, J.-P. Bibring, F. Forget, K. W. Lewis, O. Aharonson, M. Vincendon, and J. L. Bishop (2009), Testing evidence of recent hydration state change in sulfates on Mars, *J. Geophys. Res.*, *114*, E00D02, doi:10.1029/2008JE003245.
- Rodriguez-Navarro, C., and E. Doehne (1999), Salt weathering: Influence of evaporation rate, supersaturation and crystallization pattern, *Earth Surf. Processes Landforms*, *24*, 191–209, doi:10.1002/(SICI)1096-9837(199903)24:3<191::AID-ESP942>3.0.CO;2-G.
- Rossi, A. P., G. Neukum, M. Pondrelli, S. van Gassel, T. Zegers, E. Hauber, A. Chicarro, and B. Foing (2008), Large-scale spring deposits on Mars?, *J. Geophys. Res.*, *113*, E08016, doi:10.1029/2007JE003062.
- Scherer, G. W. (2004), Stress from crystallization of salt, *Cement Concr. Res.*, *34*, 1613–1624, doi:10.1016/j.cemconres.2003.12.034.
- Showman, A. P., I. Mosqueira, and J. W. Head (2004), On the resurfacing of Ganymede by liquid-water volcanism, *Icarus*, *172*, 625–640, doi:10.1016/j.icarus.2004.07.011.
- Soukhovitskaya, V., and M. Manga (2006), Martian landslides in Valles Marineris: Wet or dry?, *Icarus*, *180*, 348–352, doi:10.1016/j.icarus.2005.09.008.
- Squyres, S. W., et al. (2006), Two years at Meridiani Planum: Results from the Opportunity Rover, *Science*, *313*, 1403–1407, doi:10.1126/science.1130890.
- Steiger, M., and S. Asmussen (2008), Crystallization of sodium sulfate phases in porous materials: The phase diagram Na₂SO₄-H₂O and the generation of stress, *Geochim. Cosmochim. Acta*, *72*, 4291–4306, doi:10.1016/j.gca.2008.05.053.
- Steiger, M., K. Linnow, H. Jüling, G. Gülker, A. El Jarad, S. Brüggerhoff, and D. Kirchner (2008), Hydration of MgSO₄·H₂O and generation of stress in porous materials, *Cryst. Growth Des.*, *8*, 336–343, doi:10.1021/cg060688c.
- Turcotte, D. L., and G. Schubert (2002), *Geodynamics*, Cambridge Univ. Press, Cambridge, U. K.
- Ward, A. W. (1979), Yardangs on Mars: Evidence of recent wind erosion, *J. Geophys. Res.*, *84*, 8147–8166, doi:10.1029/JB084iB14p08147.
- Warren, J. K. (2006), *Evaporites: Sediments, Resources and Hydrocarbons*, doi:10.1007/3-540-32344-9, Springer, Berlin.
- Weitz, C. M., R. E. Milliken, J. A. Grant, A. S. McEwen, R. M. E. Williams, J. L. Bishop, and B. J. Thomson (2010), Mars Reconnaissance Orbiter observations of light-toned layered deposits and associated fluvial landforms on the plateaus adjacent to Valles Marineris, *Icarus*, *205*, 73–102, doi:10.1016/j.icarus.2009.04.017.

M. R. Balme, Planetary Science Institute Tucson, 1700 E. Fort Lowell, Ste. 106, Tucson, AZ 85719, USA.

P. M. Grindrod, Department of Earth Sciences, University College London, Gower Street, London WC1E 6BT, UK. (p.grindrod@ucl.ac.uk)